ACS Medicinal Chemistry Letters

UNIVERSITY OF BIRMINGHAM

Subscriber access provided by University of Birmingham

Letter

Design and Synthesis of Tetrazole- and Pyridine-containing Itraconazole Analogs as Potent Angiogenetic Inhibitors

Yingjun Li, Kalyan Kumar Pasunooti, Hanjing Peng, Ruo-Jing Li, Wei Q. Shi, Wukun Liu, Zhiqiang Cheng, Sarah A. Head, and Jun O. Liu

ACS Med. Chem. Lett., **Just Accepted Manuscript** • DOI: 10.1021/acsmedchemlett.9b00438 • Publication Date (Web): 08 Apr 2020

Downloaded from pubs.acs.org on April 9, 2020

Just Accepted

"Just Accepted" manuscripts have been peer-reviewed and accepted for publication. They are posted online prior to technical editing, formatting for publication and author proofing. The American Chemical Society provides "Just Accepted" as a service to the research community to expedite the dissemination of scientific material as soon as possible after acceptance. "Just Accepted" manuscripts appear in full in PDF format accompanied by an HTML abstract. "Just Accepted" manuscripts have been fully peer reviewed, but should not be considered the official version of record. They are citable by the Digital Object Identifier (DOI®). "Just Accepted" is an optional service offered to authors. Therefore, the "Just Accepted" Web site may not include all articles that will be published in the journal. After a manuscript is technically edited and formatted, it will be removed from the "Just Accepted" Web site and published as an ASAP article. Note that technical editing may introduce minor changes to the manuscript text and/or graphics which could affect content, and all legal disclaimers and ethical guidelines that apply to the journal pertain. ACS cannot be held responsible for errors or consequences arising from the use of information contained in these "Just Accepted" manuscripts.

is published by the American Chemical Society. 1155 Sixteenth Street N.W., Washington, DC 20036

Published by American Chemical Society. Copyright © American Chemical Society. However, no copyright claim is made to original U.S. Government works, or works produced by employees of any Commonwealth realm Crown government in the course of their duties.

Design and Synthesis of Tetrazole- and Pyridine-containing Itraconazole Analogs as Potent Angiogenetic Inhibitors

Yingjun Li,[†] Kalyan Kumar Pasunooti,[†,⊥] Hanjing Peng,[†] Ruo-Jing Li,[†,§] Wei Q. Shi,[†,††] Wukun Liu,[†,‡‡] Zhiqiang Cheng,[†] Sarah A. Head,[†,§§] Jun O. Liu*,[†,‡]

[†]Department of Pharmacology and Molecular Sciences, Johns Hopkins School of Medicine, Baltimore, Maryland 21205, United States

[‡]Department of Oncology, Johns Hopkins School of Medicine, Baltimore, Maryland 21205, United States

KEYWORDS: angiogenesis inhibitor, itraconazole, CYP3A4, NPC1.

ABSTRACT: Itraconazole, a widely used antifungal drug, was found to possess anti-angiogenic activity and is currently undergoing multiple clinical trials for the treatment of different types of cancer. However, it suffers from extremely low solubility and strong interactions with many drugs through inhibition of CYP3A4, limiting its potential as a new anti-angiogenic and anticancer drug. To address these issues, a series of analogs in which the phenyl group is replaced with pyridine or fluorine-substituted benzene was synthesized. Among them the pyridine- and tetrazole-containing compound **24** has significantly improved solubility and reduced CYP3A4 inhibition compared to itraconazole. Similar to itraconazole, compound **24** inhibited the AMPK/mTOR signaling axis and the glycosylation of VEGFR2. It also induced cholesterol accumulation in the endolysosome and demonstrated binding to the sterol-sensing domain of NPC1 in a simulation study. These results suggested that compound **24** may serve as an attractive candidate for the development of a new generation of anti-angiogenic drug.

Itraconazole (**1**, **Figure 1**) is a triazole-containing antifungal drug that has been found to possess anti-angiogenic activity.[1] The anti-angiogenic and anticancer activities of itraconazole have been demonstrated in animal models and it has shown efficacy in multiple phase II clinical trials for the treatment of lung cancer, prostate cancer and basal cell carcinoma.[2-4] The underlying mechanism of angiogenesis inhibition has been extensively investigated.[5] Itraconazole was found to bind two distinct molecular targets, Niemann-Pick Type C 1 (NPC1) and Voltage-Dependent Anion Channel 1 (VDAC1) in primary human umbilical vein endothelial cells (HUVECs).[6,7] NPC1, a membrane protein localized to the late endosomes and lysosomes (collectively called endolysosomes), mediates cholesterol trafficking from the endolysosome to other cellular compartments.[8] The inhibition of NPC1 by itraconazole, or the structurally related drug posaconazole, leads to the accumulation of cholesterol in the endolysosome[9,10]. VDAC1, a channel on the mitochondrial outer membrane, serves as a key gateway for a multitude of important cellular metabolites including adenosine diphosphate (ADP) and adenosine triphosphate (ATP) to enter and exit the mitochondria.[11] Inhibition of VDAC1 by itraconazole increases the AMP/ATP ratio, thereby activating the AMP-activated protein kinase (AMPK) signaling pathway in endothelial cells. Dual inhibition of NPC1 and VDAC1 culminates in a synergistic inhibition of mechanistic target of rapamycin (mTOR), blocking the proliferation of endothelial cells and angiogenesis.[9] In addition, itraconazole has also been shown to inhibit the glycosylation and trafficking of vascular endothelial growth factor receptor 2 (VEGFR2), which is also required for pathological angiogenesis.[12]

Despite its potential as a novel anti-angiogenic drug, itraconazole has three major limitations. First, the inhibition of Cytochrome P450 3A4 (CYP3A4) prevents combination therapy of itraconazole with the majority of other anticancer drugs.[13,14] Second, the high lipophilicity of itraconazole (cLogP= 5.3) results in its accumulation in adipose

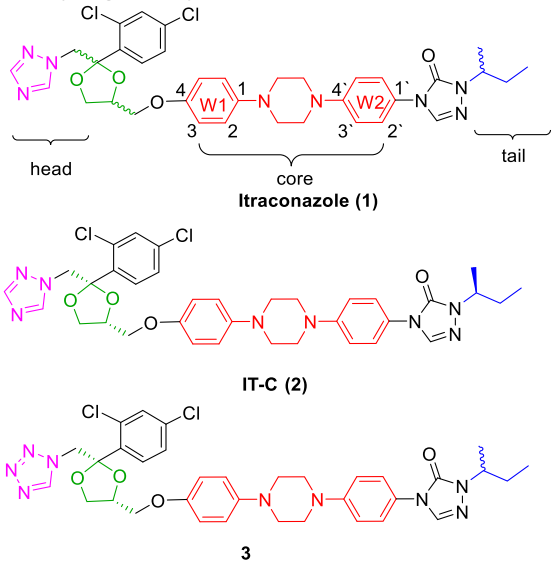

Figure 1. Structures of itraconazole (**1**), IT-C (**2**) and compound **3**.

tissues, with concentrations in skin and fat tissues to be 19-fold and 17-fold greater than that in the plasma, respectively.[15] Third, itraconazole is relatively insoluble in water and has limited oral bioavailability. Although a clinically-used suspension formulation is able to improve its bioavailability, itraconazole has a highly variable absorption and plasma concentrations from individual to individual.[16,17] The high lipophilicity and the low solubility of itraconazole, though tolerable for the treatment of fungal infections, pose major problems in the treatment of cancer.

In our attempts to improve the potency and reduce the toxicity of itraconazole, we conducted systematic structure and activity relationship (SAR) studies on the two ends of itraconazole. Compound IT-C (**2**) with cis-(2S,4R) stereochemistry in the dioxolane ring, wherein the isobutyl sidechain with a 2'S configuration, showed the strongest anti-angiogenic activity among the 8 stereoisomers of itraconazole and significantly reduced hepatotoxicity.[18,19] Compound **3** with tetrazole in place of the 1,2,4-triazole in the head position had increased activity and significantly reduced CYP3A4 inhibition while a methyl substitution in the same position resulted in the loss of anti-angiogenic activity.[20] Moreover, the sec-butyl tail (or similar alkyl group) was required for angiogenesis inhibition.[21]

Although modifications at the "head" and "tail" sections of itraconazole have effectively reduced the CYP3A4 inhibition and hepatotoxicity,[14,19] the hydrophobicity and accompanying low water solubility remains to be resolved. The hydrophobicity of itraconazole can be attributed in large part to the two phenyl groups in the "core" region of the molecule (**W1**-piperizin-1-yl-**W2**, **Figure 1**). The phenyl-piperizin-1-yl-phenyl core portion has a symmetrical and rigid configuration. It was reported that symmetrical and rigid compounds have high crystal packing energies, and therefore have low solubility in water as well as in organic solvents.[22,23] It has been shown previously that replacement of the **W2** phenyl with a pyridyl group can significantly increase the solubility and bioavailability of itraconazole analogs.[24] We took a similar approach by using pyridine to replace phenyl group or adding a fluorine substitution on the phenyl ring. The synthesis and anti-angiogenic activity characterization of the novel analogs are reported herein.

The syntheses of novel itraconazole analogs were accomplished using modified synthetic routes reported previously (**Scheme 1**).[14] Nucleophilic displacement of the bromine in **4** with 1,2,4-triazole, imidazole or tetrazole, followed by ketalization ring-closure reaction with enantiomerically pure glyceryl tosylate **6** under strong acid conditions, provided 1,3-dioxolane intermediate as a *cis*- and *trans*- mixture in a ratio of 3:1. The *cis-2S,4R* diastereomers **7a-c** were separated with column chromatograph. For

Scheme 1: Synthesis of Compounds 4, 5, 8-12 and **15-26**[a]

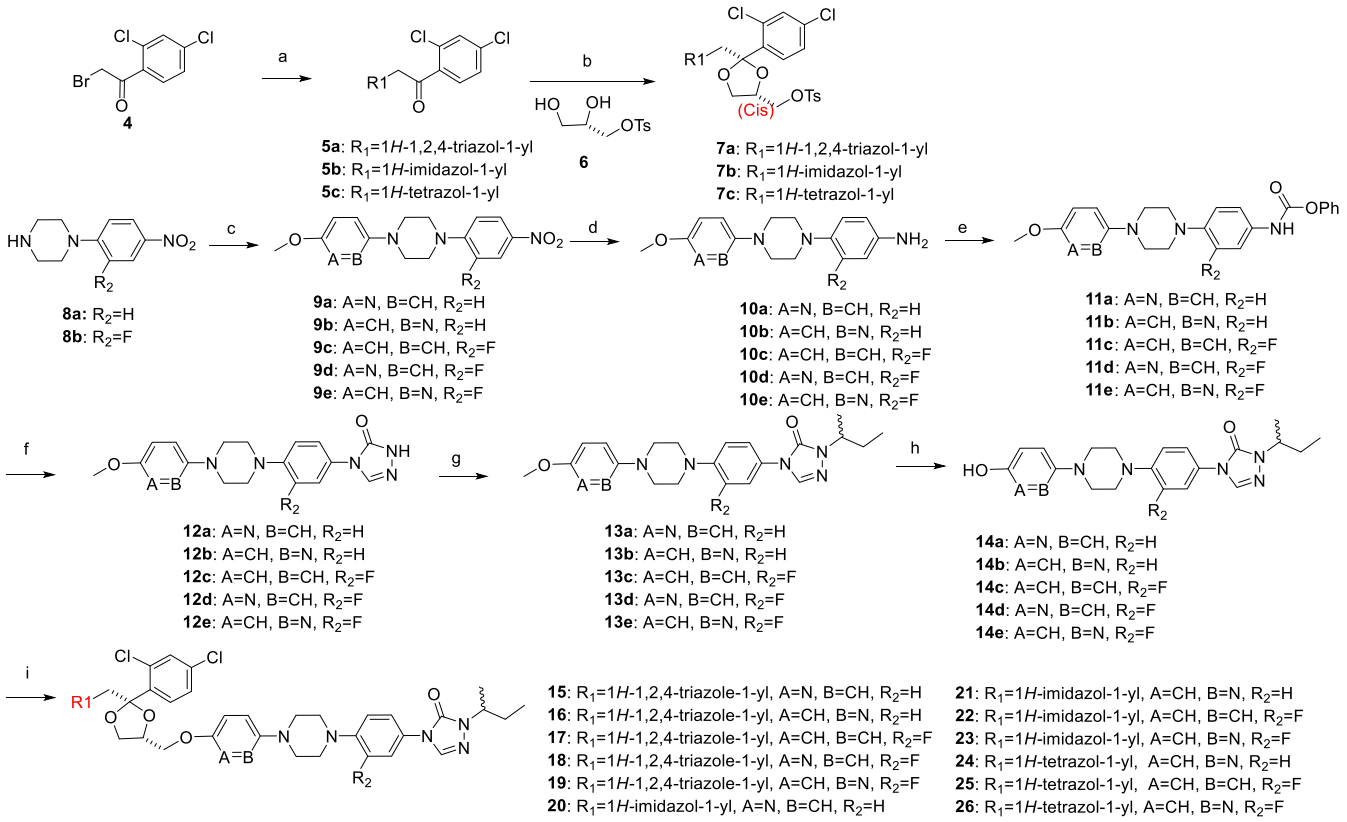

[a]Reagents and conditions: (a) azoles, K_2CO_3, MeCN, 25°C, 16 h, 40-70%; (b) **6**, TfOH, toluene, rt, 60 h, 55%; (c) $Pd_2(dba)_3$, BINAP, NaOtBu, toluene, 80 °C, 16 h, 80%; (d) 10% Pd/C, $N_2H_4.H_2O$, EtOH, reflux, 3.5h, 93%; (e) Phenyl chloroformate, pyridine, rt, 16h, 82%; (f) i.$NH_2NH_2.H_2O$, 1,4-dioxane, reflux, 3h; ii. formamidine acetate, 1-propanol, reflux, 3h, 66%; (g) 2-bromobutane, K_2CO_3, DMSO, 80 °C, 16 h, 82%; (h) 48% aqueous HBr, reflux, 76%; (i) **7a-c**, NaH, DMF, 80 °C, 16 h, 60-75%.

analogs in which the **W1** group was a pyridyl, Buchwald-Hartwig cross coupling of bromides with **8a-b** was used to generate nitrobenzene **9a-e**.[25] Then the nitro group was reduced to an amine with 10% Pd/C and hydrazine monohydrate in ethanol. The triazolone ring was built in three steps by reacting the aniline intermediates with phenyl chloroformate, hydrazine monohydrate, and formamidine acetate, successively.[20] N-alkylation of triazolone **12a-e** with 2-bromobutane under basic conditions afforded the intermediates **13a-e**. The methyl protecting group in **13a-e** was unmasked with 48% aqueous hydrobromic acid (HBr). The resulting phenol **14a-e** was coupled with tosylate **7a-c** to give the desired compounds **15-26**. Compounds **27-30** were synthesized under similar conditions (**Supplementary Scheme 1**). All desired compounds were evaluated as racemic mixtures (2-*S*-butanyl group and 2-*R*-butanyl group) for their biological activities.

The inhibitory effects of the new analogs on HUVEC proliferation were determined using a [^{3}H]-thymidine incorporation assay.[26] The cLogP values, used as an indicator of lipophilicity, were calculated using ALOGPS2.1 software. Aqueous solubility is a key physiochemical property relevant for oral absorption. We determined the solubility of each analog in 0.001 N HCl (pH = 3), which is similar to that in the acidic human gastric fluid.[22,27] The IC_{50} values for inhibition of HUVEC proliferation, cLogP and solubility of all analogs are shown in **Table 1**. Itraconazole was slightly soluble in 0.001N HCl (10.1 ng/mL). In order to disrupt the symmetricity of the phenyl-piperizin-1-yl-phenyl core (**W1-** piperizin-1-yl-**W2**), we used pyridyl moiety to replace one of the two phenyl rings in the **W1** or **W2** position or 3`-fluorophenyl to replace **W2.** Both pyridine and fluoro-benzene are reasonable benzene isosteres and were not expected to cause significant steric perturbations of the **W1**-**W2** portion of the molecules. Initially, compounds **15-19, 27** and **28** with 1,2,4-triazole in the $\mathbf{R_1}$ position were synthesized and characterized. Pyridyl substitution at either the **W1** (**15**, **16**) or **W2** (**27**, **28**) position and 3`-fluoro-phenyl at **W2** (**17-19**) all resulted in increases in solubility by 5-84 folds. The pyridin-2-yl and 3`-fluorophenyl combination (**19**) resulted in the best solubility in this series of analogs (847.7 ng/mL). Pyridine (=N), benzene (=CH), and fluorine-substituted benzene (=CF) are similar in van der Waals radius but quite different in lipophilicity.[28] The lipophilicity of the three groups follows the order: pyridyl < benzyl < fluoro-benzyl.[29] As expected, the analogs containing a pyridine (**15, 16, 27, 28**) exhibited decreases in cLogP, while the fluoro-phenyl analog (**17**) had an increased clogP. In the HUVEC proliferation assay, compounds **28, 17**, and **19** showed similar activity to that of itraconazole, while the other modifications led to decreases in potency.

Next, six analogs with imidazole in the $\mathbf{R_1}$ position were synthesized and characterized. Except for compound **20** (pyridin-3-yl) and **30** (pyridin-2'-yl), the other four analogs (**21**, **29**, **22**, **23**) exhibited increased activities for inhibition of HUVEC proliferation. In general, replacement of the triazole with an imidazole led to a significant increase in solubility ranging from 6 μg/mL to 125 μg/mL, much greater than itraconazole. However, the imidazole compounds were more lipophilic (higher cLogP value) than

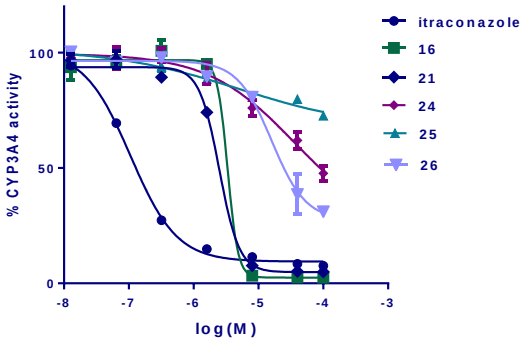

Figure 2. Dose-response curves of CYP3A4 enzyme inhibition by itraconazole (**1**) and analogs **5**, **12**, **24**, **25** and **26**.

their 1,2,4-triazole counterparts, which was unfavorable for drug distribution. Moreover, the 1,2,4-triazole- and imidazole-containing compounds displayed inhibition of CYP3A4, albeit weaker than itraconazole. For example, the IC_{50} of compounds **16** and **21** for CYP3A4 inhibition were 3.4 μM and 2.6 μM, respectively. (**Figure 2**).

Our previous SAR study showed that 1*H*-tetrazole-1-yl in the $\mathbf{R_1}$ position significantly reduced CYP3A4 inhibition and increased anti-angiogenic potency.[14] Thus, three new analogs with either pyridin-2-yl, 3`-fluorophenyl or the combination in the core region and tetrazole in the $\mathbf{R_1}$ position were synthesized. As expected, the resulting tetrazole-containing analogs had reduced CYP3A4 inhibition and the IC_{50} values of **24** and **25** are greater than 90 μM (**Figure 2**). To our delight, the calculated logP values of the three new analogs were further decreased and the clogP of **24** was reduced to 4.36, falling into the range of orally active drugs according to Lipinski`s rule of five.[30] Among the three tetrazole-containing analogs, compound **24** also had the highest potency for HUVEC inhibition (IC_{50} of 77 nM) and highest solubility. Compared to itraconazole, the solubility of **24** was increased by over 90-fold.

Tetrazole compounds **24** and **26** were selected for endothelial cell tube formation assay to further assess their anti-angiogenic potential, with compound **3** as a positive

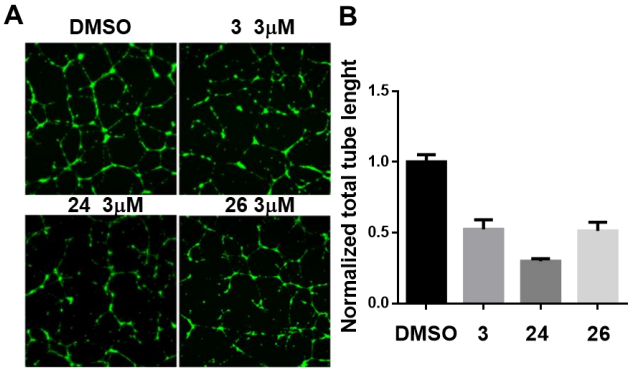

Figure 3. Inhibition of HUVEC tube formation. HUVECs were seeded on Matrigel-coated plates and treated with DMSO or 3μM of **3**, **24** and **26** for 24h. (**A**) Cells were stained with Calcein-AM and vascular networks were imaged using fluorescence microscopy. (**B**) Quantified total tube lengths from the fluorescence images. Data represent mean ± SD of three independent experiments.

Table 1: Inhibition of HUVEC Proliferation, Aqueous Solubility and cLogP of Itraconazole Analogs

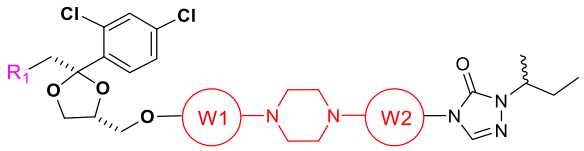

	R_1	W1	W2	HUVEC inhibition[a] IC_{50} (nM)	cLogP[b]	Solubility in 0.001N HCl[c] (ng/mL)
1				**170** ± 13.1	5.35	10.1
3				**73** ± 17.0	4.92	321.4
15		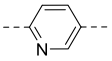	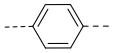	**686.8** ± 78.1	5.00	116.1
16		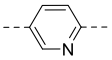	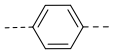	**379.8** ± 50.8	4.99	113.6
27		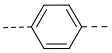	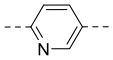	**221.9** ± 23.1	5.02	53.9
28		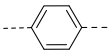	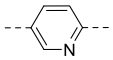	**187.8** ± 17.5	5.04	496.5
17		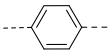	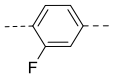	**128.4** ± 59.7	5.75	29.1
18		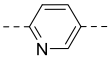	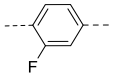	**446.5** ± 38.3	5.12	255.4
19		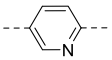	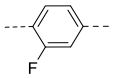	**173.1** ± 27.6	5.11	847.7
20		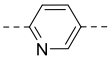	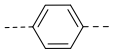	**468.5** ± 42.2	5.48	6483.0
21		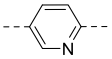	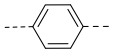	**69.1** ± 7.0	5.47	2938.9
29		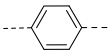	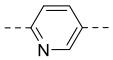	**98.5** ± 36.3	5.49	7988.0
30		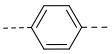	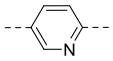	**636.0** ± 177.2	5.52	41338.6
22		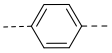	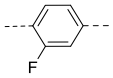	**70.1** ± 15.4	6.16	17150.0
23		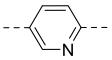	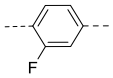	**68.0** ± 15.5	5.61	124904.5
24		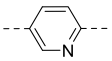	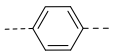	**77.1** ± 11.9	4.36	951.3
25		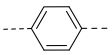	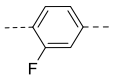	**153.4** ± 32.7	4.96	52.8
26		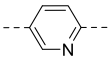	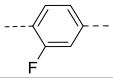	**108.5** ± 8.6	4.40	707.6

[a]IC_{50} in HUVEC was evaluated using [^{3}H]-thymidine incorporation assay. Values represent the mean ± SD in three independent experiments carried out in triplicate; [b] cLogP was the calculated partition coefficient between n-octanol and water $\log(c_{octanol}/c_{water})$ using ALOGPS2.1 software; [c]The thermodynamic solubility in 0.001N HCl was measured using HPLC.

control. In this assay, HUVEC assembled into three-dimensional networks and formed tubular structures in Matrigel-coated wells, recapitulating many key aspects of new blood vessel formation in vivo. Compound **24** inhibited 70% of HUVEC tube formation at 3 μM, as judged by total tube length, further demonstrating its anti-angiogenetic potency (**Figure 3**).

NPC1 plays an essential role in cholesterol export from the endolysosome.[31] Previously, we and others reported itraconazole and its structurally related drug posaconazole

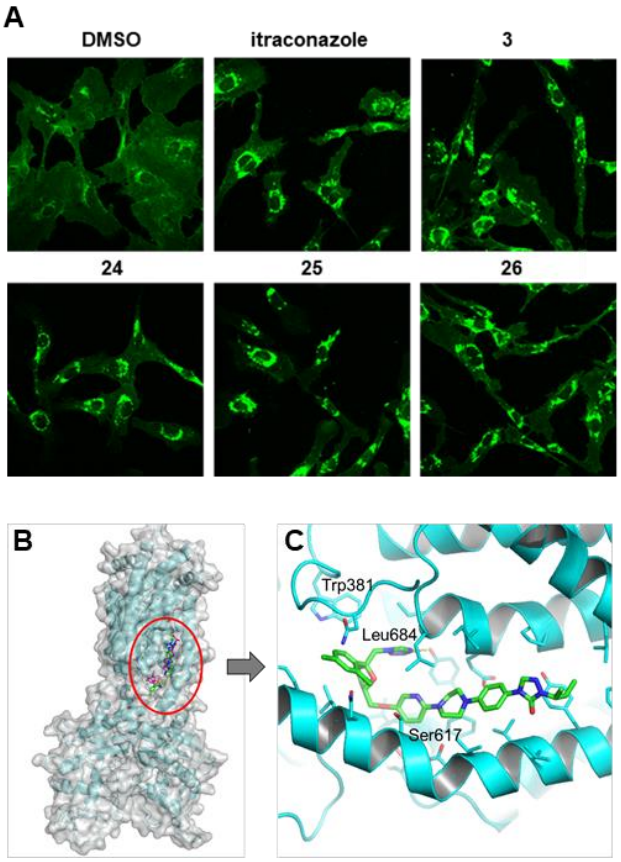

Figure 4. Inhibition of NPC1. (**A**): HUVECs were treated with 0.2 μM **itraconazole**, **3, 24, 25, 26** or DMSO for 24 h. Intracellular cholesterol was stained with filipin and fluorescent images were captured using LSM710 confocal microscope with 25x objective. Predicted binding mode of itraconazole (magenta) and **24** (green) with NPC1 (PDB code: 5I31) by AutoDock Vina software (**B**). The predicted interaction of compound **24** (green) with SSD (**C**).

target NPC1 and induce NPC phenotype in endothelial cells.[9,10] Using filipin staining, we observed that compound **24** caused a massive build-up of cholesterol in the perinuclear structure, in the same manner as itraconazole and the other tetrazole-containing analogs **3**, **25** and **26** (**Figure 4A**).[7] These results suggested that the pyridinyl and fluorophenyl analogs retained NPC1 inhibitory activity of itraconazole. To further assess the potential binding of **24** to NPC1 protein, we performed docking of compound **24** and itraconazole into the pocket within the sterol-sensing domain (SSD) using AutoDock Vina software as we have previous shown that itraconazole binds to the SSD domain of NPC1.[7,32] As shown in **Figure 4B**, itraconazole and **24** were predicted to bind to NPC1 in a similar manner. The linear pyridinyl-piperizin-1-yl-phenyl core of **24** nestled into the hydrophobic channel created by the transmembrane helices (**Figure 4C**). The isobutyl tail faced the open entrance of this channel. The tetrazole moiety pointed to the closed end of the pocket and interacted with the hydroxyl group of Tyr1225 via hydrogen bonding. These results offered a plausible explanation of how the benzene bioisostere replacement could modify the physiochemical properties of itraconazole without compromising NPC1 inhibition.

Next, we determined the effects of **24** on AMPK/mTOR activity and VEGFR2 glycosylation. Similar to itraconazole, **24** activated AMPK as judged by the phosphorylation of its substrate acetyl CoA carboxylase (ACC) in a dose-dependent manner (**Figure 5A**). AMPK activation and NPC1 inhibition were demonstrated to lead to synergistic mTOR inhibition by itraconazole.[33] Indeed, **24** potently inhibited the phosphorylation of the mTOR substrate p70 S6 Kinase (S6K) in a dose-dependent manner.

We have previously shown that itraconazole inhibits VEGFR2 glycosylation and surface expression.[12] We observed two VEGFR2 bands by Western blotting, representing differentially glycosylated forms of the receptor, with the higher molecular weight band being more predominant in untreated HUVEC. Treatment with **24** caused a mobility shift to the lower molecular weight, hypoglycosylated band. The high molecular weight species of VEGFR2 disappeared upon treatment with **24** at 0.5 μM or higher concentrations (**Figure 5A**). We next determined whether **24** and other

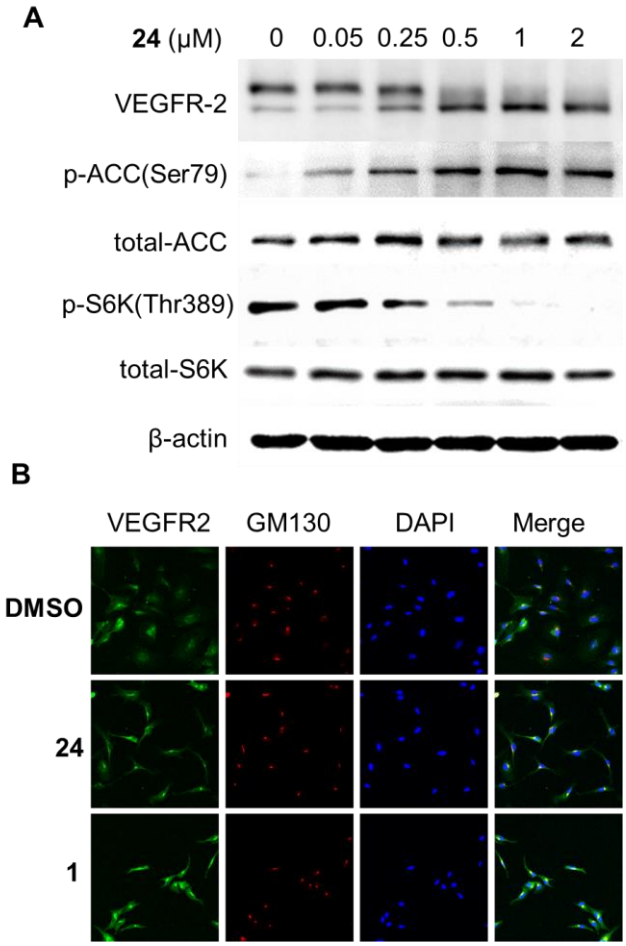

Figure 5. Inhibition of VEGFR2 and AMPK/mTOR in HUVEC. (**A**) HUVECs were treated with 0.05μM, 0.25μM, 0.5μM, 1μM or 2μM **24** or DMSO for 24 h. VEGFR2, p-ACC, total-ACC, p-S6K, total S6K and β-actin proteins were analyzed by western blot. (**B**) HUVECs were treated with DMSO, 2μM compound **24** or itraconazole (**1**). The cells were stained with VEGFR2 (green), GM130 (red) antibody and DAPI (blue). Images were captured using LSM 700 confocal microscopy.

analogs affected cellular localization of VEGFR2 using immunofluorescence staining (**Figure 5B**). In **24** and itraconazole-treated cells, VEGFR2 accumulated in the perinuclear region and colocalized with the Golgi marker, GM130. In contrast, in the untreated cells, VEGFR2 uniformly distributed in small puncta throughout the cytoplasm. As a critical component of lipid rafts, cholesterol is pivotal to intracellular transport and cell signaling. In our previous study, we demonstrated that the hypoglycosylation of VEGFR2 was rescued by supplementation with exogenous cholesterol. It is therefore possible that VEGFR2 relocalization and inhibition by itraconazole and its analogs may be mediated through inhibition of NPC1. Taken together, these results indicated that **24**, like itraconazole, inhibits endothelial cell growth and angiogenesis by concurrent inhibition of NPC1 and VDAC1, leading to activation of AMPK, and inhibition of mTOR and VEGFR2 signaling.

Anti-angiogenic therapy has been clinically validated for the treatment of a number of diseases including cancer, autoimmune disorders, retinopathy, obesity, macular degeneration and others.[34] Itraconazole has great potential as a newly identified angiogenesis inhibitor and is under investigation in multiple clinical trials. However, its wider use as an anti-angiogenic agent in general, and its use in combination with other drugs for treating cancer in particular, has been limited by its inhibition of CYP450 and unfavorable physicochemical properties. To improve its solubility and decrease its lipophilicity, we used pyridyl or fluorophenyl groups to replace the phenyl group in the core region of itraconazole. Among the newly synthesized analogs, **24** with 2-pyridyl in **W1** and 1*H*-tetrazol-1-yl in $\mathbf{R_1}$ position exhibited improved anti-angiogenic activity, solubility and hydrophilicity with negligible effects on CYP3A4. The anti-angiogenic activity of **24** was further validated using a tube formation assay. Moreover, **24** bears all the hallmarks of itraconazole activity in endothelial cells, including activation of AMPK and inhibition of mTOR, induction of cholesterol accumulation in the endolysosome and binding to NPC1, and inhibition of VEGFR2 glycosylation, suggesting that the structural changes required to improve its pharmacological properties did not alter its mechanism of action. This work paves the way for **24** to undergo further preclinical studies as a novel anti-angiogenic and anticancer drug candidate.

ASSOCIATED CONTENT

Supporting Information

The Supporting Information is available free of charge on the ACS Publications website.

Synthetic procedures, assay protocols, concentration standard curve of **24**, IC_{50} of CYP3A4 inhibition, western blot of itraconazole and analytical data (PDF)

AUTHOR INFORMATION

Corresponding Author

*Phone, 410-955-4619; fax, 410-955-4520; e-mail, joliu@jhu.edu

Present Addresses

⊥ProSAMBio, Hyderabad,Telangana500049, India
§FDA, Silver Spring, Maryland 20993, United States
††Department of Chemistry, Ball State University, Muncie, Indiana 47306, United States
‡‡Nanjing University of Chinese Medicine,Jiangsu, Nanjing210023, China,
§§Centre for Genomic Regulation (CRG), The Barcelona Institute of Science and Technology, Barcelona 08003, Spain

Author Contributions

The manuscript was written through contributions of all authors. All authors have given approval to the final version of the manuscript.

Funding Sources

This work was supported by the National Cancer Institutes (Grant R01CA184103) and the Flight Attendant Medical Research Institute.

Notes

The authors declare no competing financial interest.

ABBREVIATIONS

HUVEC, human umbilical vein endothelial cell; NPC1, Niemann-Pick disease, type C1; VDAC1, voltage-dependent anion channel 1; AMPK, AMP-activated protein kinase; ATP, adenosine triphosphate; ADP, adenosine diphosphate; mTORC, mammalian target of rapamycin complex; CYP3A4, cytochrome P450 3A4; SAR, structure-activity relationship; VEGFR, vascular endothelial growth factor receptor; IC_{50}, half-maximal inhibitory concentration; DMSO, dimethyl sulfoxide; DMF, dimethylformamide; HBr, hydrobromic acid; THF, tetrahydrofuran; DCM, dichloromethane; TfOH, trifluoromethanesulfonic acid; NaH, sodium hydride; SSD, sterol-sensing domain; ACC, acetyl CoA carboxylase; S6K, p70 S6 kinase; δ, chemical shifts; MeCN, acetonitrile; $Pd_2(dba)_3$, tris(dibenzylideneacetone)dipalladium; EtOAc, ethyl acetate; NaOtBu, sodium t-butoxide; BINAP, 2,2′-bis(diphenyl phosphino)-1,1′-binaphthalene.

REFERENCES

(1) Chong, C. R.; Xu, J.; Lu, J.; Bhat, S.; Sullivan, D. J., Jr.; Liu, J. O. Inhibition of angiogenesis by the antifungal drug itraconazole. *ACS Chem. Biol.* **2007,** 2, 263-270.
(2) Kim, D. J.; Kim, J.; Spaunhurst, K.; Montoya, J.; Khodosh, R.; Chandra, K.; Fu, T.; Gilliam, A.; Molgo, M.; Beachy, P. A.; Tang, J. Y. Open-label, exploratory phase II trial of oral itraconazole for the treatment of basal cell carcinoma. *J Clin Oncol.***2014,** 32, 745-751.
(3) Rudin, C. M.; Brahmer, J. R.; Juergens, R. A.; Hann, C. L.; Ettinger, D. S.; Sebree, R.; Smith, R.; Aftab, B. T.; Huang, P.; Liu, J. O. Phase 2 study of pemetrexed and itraconazole as second-line therapy for metastatic nonsquamous non-small-cell lung cancer. *J Thorac Oncol.* **2013,** 8, 619-623.
(4) Antonarakis, E. S.; Heath, E. I.; Smith, D. C.; Rathkopf, D.; Blackford, A. L.; Danila, D. C.; King, S.; Frost, A.; Ajiboye, A. S.; Zhao, M.; Mendonca, J.; Kachhap, S. K.; Rudek, M. A.; Carducci, M. A. Repurposing itraconazole as a treatment for advanced prostate cancer: a noncomparative randomized phase II trial in men with metastatic castration-resistant prostate cancer. *Oncologist* **2013,** 18, 163-173.
(5) Shim, J. S.; Liu, J. O. Recent advances in drug repositioning for the discovery of new anticancer drugs. *Int J Biol Sci.* **2014,** 10, 654-663.
(6) Head, S. A.; Shi, W.; Zhao, L.; Gorshkov, K.; Pasunooti, K.; Chen, Y.; Deng, Z.; Li, R. J.; Shim, J. S.; Tan, W.; Hartung, T.; Zhang, J.; Zhao, Y.; Colombini, M.; Liu, J. O. Antifungal drug itraconazole targets

VDAC1 to modulate the AMPK/mTOR signaling axis in endothelial cells. *Proc Natl Acad Sci U S A.* **2015,** 112, 7276-7285.
(7) Head, S. A.; Shi, W. Q. Simultaneous targeting of NPC1 and VDAC1 by itraconazole leads to synergistic inhibition of mTOR signaling and angiogenesis. *ACS Chem Biol.***2017,** 12, 174-182.
(8) Infante, R. E.; Wang, M. L.; Radhakrishnan, A.; Kwon, H. J.; Brown, M. S.; Goldstein, J. L. NPC2 facilitates bidirectional transfer of cholesterol between NPC1 and lipid bilayers, a step in cholesterol egress from lysosomes. *Proc Natl Acad Sci U S A.* **2008,** 105, 15287-15292.
(9) Xu, J.; Dang, Y.; Ren, Y. R.; Liu, J. O. Cholesterol trafficking is required for mTOR activation in endothelial cells. *Proc Natl Acad Sci U S A.* **2010,** 107, 4764-4769.
(10) Trinh, M. N.; Lu, F.; Li, X.; Das, A.; Liang, Q.; De Brabander, J. K.; Brown, M. S.; Goldstein, J. L. Triazoles inhibit cholesterol export from lysosomes by binding to NPC1. *Proc Natl Acad Sci U S A.* **2017,** 114, 89-94.
(11) Shoshan-Barmatz, V.; De Pinto, V.; Zweckstetter, M.; Raviv, Z.; Keinan, N.; Arbel, N. VDAC, a multi-functional mitochondrial protein regulating cell life and death. *Mol Aspects Med* **2010,** 31, 227-285.
(12) Nacev, B. A.; Grassi, P.; Dell, A.; Haslam, S. M.; Liu, J. O. The antifungal drug itraconazole inhibits vascular endothelial growth factor receptor 2 (VEGFR2) glycosylation, trafficking, and signaling in endothelial cells. *J Biol Chem* **2011,** 286, 44045-4456.
(13) Isoherranen, N.; Kunze, K. L.; Allen, K. E.; Nelson, W. L.; Thummel, K. E. Role of itraconazole metabolites in CYP3A4 inhibition. *Drug Metab Dispos* **2004,** 32, 1121-1131.
(14) Li, Y.; Pasunooti, K. K.; Li, R.-J.; Liu, W.; Head, S. A.; Shi, W. Q.; Liu, J. O. Novel Tetrazole-containing analogues of itraconazole as potent antiangiogenic agents with reduced Cytochrome P450 3A4 inhibition. *J Med Chem.* **2018,** 61, 11158-11168.
(15) Willems, L.; van der Geest, R.; de Beule, K. Itraconazole oral solution and intravenous formulations: a review of pharmacokinetics and pharmacodynamics. *J Clin Pharm Ther.* **2001,** 26, 159-169.
(16) Bellmann, R.; Smuszkiewicz, P. J. I. Pharmacokinetics of antifungal drugs: practical implications for optimized treatment of patients. *Infection***2017,** 45, 737-779.
(17) Goodwin, M. L.; Drew, R. H. Antifungal serum concentration monitoring: an update. *J Antimicrob Chemother.* **2008,** 61, 17-25
(18) Shi, W.; Nacev, B. A.; Bhat, S.; Liu, J. O. Impact of absolute stereochemistry on the antiangiogenic and antifungal activities of itraconazole. *ACS Med Chem Lett.***2010,** 1, 155-159.
(19) Shim, J. S.; Li, R. J.; Bumpus, N. N.; Head, S. A.; Kumar Pasunooti, K.; Yang, E. J.; Lv, J.; Shi, W.; Liu, J. O. Divergence of antiangiogenic activity and hepatotoxicity of different stereoisomers of itraconazole. *Clin Cancer Res.***2016,** 22, 2709-2720.
(20) Pace, J. R.; DeBerardinis, A. M.; Sail, V.; Tacheva-Grigorova, S. K.; Chan, K. A.; Tran, R.; Raccuia, D. S.; Wechsler-Reya, R. J.; Hadden, M. K. Repurposing the clinically efficacious antifungal agent itraconazole as an anticancer chemotherapeutic. *J Med Chem.* **2016,** 59, 3635-3649.
(21) Shi, W.; Nacev, B. A.; Aftab, B. T.; Head, S.; Rudin, C. M.; Liu, J. O. Itraconazole side chain analogues: structure-activity relationship studies for inhibition of endothelial cell proliferation, vascular endothelial growth factor receptor 2 (VEGFR2) glycosylation, and hedgehog signaling. *J Med Chem.* **2011,** 54, 7363-7374.
(22) Ishikawa, M.; Hashimoto, Y. Improvement in aqueous solubility in small molecule drug discovery programs by disruption of molecular planarity and symmetry. *J Med Chem.* **2011,** 54, 1539-1554.
(23) Pinal, R. Effect of molecular symmetry on melting temperature and solubility. *Org Biomol Chem.***2004,** 2, 2692-2699.
(24) Liu, Y.; Liu, Z.; Cao, X.; Liu, X.; He, H.; Yang, Y. Design and synthesis of pyridine-substituted itraconazole analogues with improved antifungal activities, water solubility and bioavailability. B*ioorg. Med. Chem. Lett* **2011,** 21, 4779-4783.
(25) Ruiz-Castillo, P.; Buchwald, S. L. Applications of palladium-catalyzed C–N cross-coupling reactions. *Chem Rev.* **2016,** 116, 12564-12649.
(26) Lyu, J.; Yang, E. J.; Head, S. A.; Ai, N.; Zhang, B.; Wu, C.; Li, R.-J.; Liu, Y.; Yang, C.; Dang, Y.; Kwon, H. J.; Ge, W.; Liu, J. O.; Shim, J. S. Pharmacological blockade of cholesterol trafficking by cepharanthine in endothelial cells suppresses angiogenesis and tumor growth. *Cancer lett.* **2017,** 409, 91-103.
(27) Shoghi, E.; Fuguet, E.; Bosch, E.; Ràfols, C. Solubility–pH profiles of some acidic, basic and amphoteric drugs. *Eur J Pharm Sci.* **2013,** 48, 291-300.
(28) Shah, P.; Westwell, A. D. The role of fluorine in medicinal chemistry. *J Enzyme Inhib Med Chem.***2007,** 22, 527-540.
(29) Polêto, M. D.; Rusu, V. H.; Grisci, B. I.; Dorn, M.; Lins, R. D.; Verli, H. Aromatic rings commonly used in medicinal chemistry: Force fields comparison and interactions with water toward the design of new chemical entities. *Front Pharmacol.* **2018,** 9, 395-395.
(30) Wang, H.-L.; Katon, J.; Balan, C.; Bannon, A. W.; Bernard, C.; Doherty, E. M.; Dominguez, C.; Gavva, N. R.; Gore, V.; Ma, V.; Nishimura, N.; Surapaneni, S.; Tang, P.; Tamir, R.; Thiel, O.; Treanor, J. J. S.; Norman, M. H. Novel Vanilloid Receptor-1 Antagonists: 3. The identification of a second-generation clinical candidate with improved physicochemical and pharmacokinetic properties. *J Med Chem.* **2007,** 50, 3528-3539.
(31) Lyu, J.; Yang, E. J.; Shim, J. S. Cholesterol trafficking: An emerging therapeutic target for angiogenesis and cancer. *Cells* **2019,** 8, 389.
(32) Li, X.; Lu, F.; Trinh, M. N.; Schmiege, P.; Seemann, J.; Wang, J.; Blobel, G. 3.3 Å structure of Niemann–Pick C1 protein reveals insights into the function of the C-terminal luminal domain in cholesterol transport. *Proc Natl Acad Sci U S A.* **2017,** 114, 9116-9121.
(33) Castellano, B. M.; Thelen, A. M.; Moldavski, O.; Feltes, M.; van der Welle, R. E. N.; Mydock-McGrane, L.; Jiang, X.; van Eijkeren, R. J.; Davis, O. B.; Louie, S. M.; Perera, R. M.; Covey, D. F.; Nomura, D. K.; Ory, D. S.; Zoncu, R. Lysosomal cholesterol activates mTORC1 via an SLC38A9-Niemann-Pick C1 signaling complex. *Science* **2017,** 355, 1306-1311.
(34) Carmeliet, P.; Jain, R. K. Angiogenesis in cancer and other diseases. *Nature* **2000,** 407, 249-257.

Insert Table of Contents artwork here